Microscopic Findings in Primary Teeth Associated with Vitamin D Deficiency

A. Allam[1*], A. C. Ionescu[2], P. Savadori[3], V. Zambelli[4], C. Salerno[5], S. Cirio[6], M. G. Cagetti[7]

[1] Department of Biomedical, Surgical and Dental Sciences, University of Milan, Milan, Italy. ORCID: 0009-0009-1988-1809
[2] Oral Microbiology and Biomaterials Laboratory, Department of Biomedical, Surgical and Dental Sciences, University of Milan, Milan, Italy; Fondazione IRCCS Cà Granda Ospedale Maggiore Policlinico, Milan, Italy. ORCID: 0000-0001-9051-4109
[3] Department of Surgery, Medicine, Dentistry and Morphological Sciences with Transplant Surgery, Oncology and Regenerative Medicine Relevance (CHIMOMO), University of Modena and Reggio Emilia, 42124 Modena, Italy; Center for Verification and Research of New Technologies in Dentistry (CRIO), University of Modena and Reggio Emilia, 42124 Modena, Italy.
[4] School of Medicine and Surgery, Università Degli Studi di Milano Bicocca, Monza, Italy.
[5] Department of Biomedical, Surgical and Dental Sciences, University of Milan, Milan, Italy; Department of Restorative, Preventive and Pediatric Dentistry, School of Dental Medicine, University of Bern, 3012 Bern, Switzerland. ORCID: 0000-0002-7799-5451
[6] Department of Biomedical, Surgical and Dental Sciences, University of Milan, Milan, Italy. ORCID: 0000-0002-3531-2595
[7] Department of Biomedical, Surgical and Dental Sciences, University of Milan, Milan, Italy. ORCID: 0000-0002-2704-0585

DOI 10.23804/ejpd.2026.2566

email: aesha.allam@unimi.it

Abstract

Background Rickets is a medical condition caused by vitamin D deficiency, typically caused by inadequate dietary intake, limited sun exposure, or, less commonly, genetic disorders. While skeletal abnormalities are the hallmark of rickets in children, oral manifestations, such as recurrent dental abscesses occurring in the absence of carious lesions, can also be observed. This report describes the case of a child presenting with oral features suggestive of hereditary rickets, despite the lack of skeletal abnormalities and without a confirmed genetic aetiology. Histological and microstructural analyses of dental tissues played a key role in guiding the diagnosis, ultimately leading to referral to a paediatrician and confirmation of vitamin D deficiency.

Case Report A 4-year-old male presented to the Emergency Dental Department of a paediatric clinic with a history of spontaneous dental abscesses. Three affected primary teeth, extracted for clinical reasons, were comprehensively analysed using micro-computed tomography, scanning electron microscopy, energy-dispersive X-ray spectroscopy, and optical microscopy. Investigations revealed an enlarged pulp chamber, pulpal calcifications, extensive interglobular dentine, and porous, hypomineralised enamel. Additionally, an irregular and poorly defined dentino-enamel junction was observed, along with abrupt spatial variations in mineral composition. The findings are consistent with defective biomineralisation. Subsequent biochemical testing confirmed vitamin D deficiency in the absence of a detectable genetic cause. The patient was supplemented with vitamin D and calcium, resulting in clinical improvement.

Conclusions Vitamin D deficiency profoundly impairs the development and mineralisation of dental hard tissues, including both enamel and dentine. These alterations compromise the structural integrity of teeth and may increase the risk of spontaneous dental abscesses. Early identification of such oral manifestations is critical for prompt diagnosis and appropriate management.

KEYWORDS Rickets, vitamin D deficiency, dental manifestations, histological analysis, micro-CT, hypomineralisation.

Introduction

Vitamin D is a fat-soluble secosteroid hormone essential for the regulation of calcium (Ca) and phosphate (P) homeostasis. It is thus critical for the development and maintenance of mineralised tissues, including bone, enamel, and dentine [Van Leeuwen et al., 2001]. Adequate serum levels of vitamin D are necessary to ensure effective intestinal absorption of calcium, thereby promoting proper mineralisation of both the skeletal system and dental structures during growth and development.

Vitamin D deficiency (hypovitaminosis D) is a widespread condition globally [Charoenngam et al., 2022]. Its prevalence varies considerably, shaped by a complex interplay of socioeconomic, cultural, and environmental determinants. In industrialised countries, the incidence has markedly declined over the last century, primarily due to food fortification initiatives and public health measures [Cashman, 2022]. In Italy, it affects approximately 79.5% of adolescents, underscoring a persisting public health concern despite the country's favourable latitude [Vierucci et al., 2013]. Vitamin D deficiency may arise from nutritional deficiencies, inadequate sunlight exposure, or genetic disorders that impair vitamin D metabolism or phosphate regulation [Holick & Chen, 2008]. Although frequently asymptomatic, it can present with non-specific clinical signs such as fatigue, diffuse bone pain, and proximal muscle weakness [Charoenngam et al., 2022]. In paediatric populations, prolonged deficiency may lead to rickets, a well-recognised clinical consequence characterised by defective mineralisation of growing bone and cartilage, resulting in skeletal deformities, delayed growth, and, in some cases, dental anomalies [Chanchlani et al., 2020]. The clinical presentation in children varies with the severity of the deficiency: while some may remain asymptomatic, others may develop a wide range of signs, including skeletal deformities, growth retardation, and muscle weakness [Haffner et al., 2021]. Vitamin D deficiency has also been associated with an increased risk of dental caries in both primary and permanent dentition [Durá-Travé & Gallinas-Victoriano, 2024]. In severe cases, such as rickets, dental manifestations may include spontaneous and recurrent dental abscesses, often occurring in the absence of carious lesions. Additional oral findings include developmental defects of enamel (DDE), dentine malformations, and altered crown-to-root ratios, which are particularly prominent in the deciduous dentition [Allam et al., 2025]. Such features reflect the impact of disrupted mineral homeostasis during critical periods of tooth development. This paper describes the case of a child presenting with recurrent dental abscesses, which necessitated the extraction of multiple deciduous teeth. Three extracted incisors underwent microscopic analysis, revealing distinct microstructural dental alterations that prompted further paediatric evaluation.

Case report

A 4-year-old male of Chinese descent presented to the Dental Clinic of the ASST Santi Paolo e Carlo Hospital (Dental Emergency

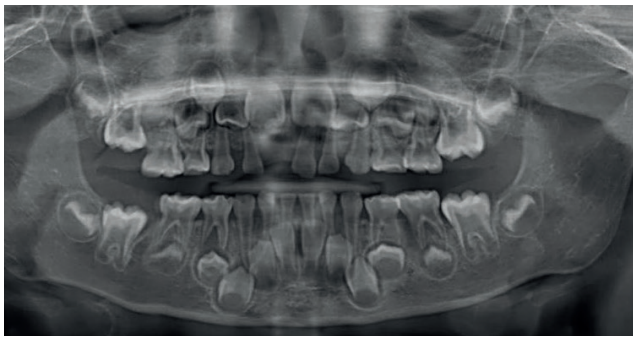

FIG. 1 Orthopantomogram shows abnormal dental morphology with large pulp chambers in all deciduous teeth as well as in the first permanent molars. The sequence of tooth eruption and formation is compatible with the patient's chronological age.

Biochemical test	Baseline	Post-treatment	Reference range
Alkaline phosphatase U/L	444	306	5-269
Calcium, mg/dL	10.2	10.4	8.8-10.8
Phosphate, mg/dL	2.8	3.1	3.3-5.6
Vitamin D 25-OH, ug/L	<9	28.7	<20 deficiency
			20-30 suboptimal
			30-100 optimal

TAB. 1 Biochemical parameters at baseline and post-treatment (9 months later).

Department) at the University of Milan, Italy, with pain localised at the fourth quadrant. According to the mother, the child had been previously hospitalised for facial cellulitis and was treated exclusively with antibiotics approximately one month prior. The dental history was also notable for recurrent dental abscesses, which had led to the extraction of tooth 5.1. Clinical examination revealed no carious lesions; however, a draining fistula was noted in association with tooth 8.1. An orthopantomogram was obtained (Figure 1), confirming the need to extract the affected tooth. Radiographic imaging also revealed abnormal dental morphology and enlarged pulp chambers involving multiple deciduous teeth. These findings, in conjunction with the history of recurrent abscesses, raised clinical suspicion of an underlying systemic or developmental condition and prompted referral for a comprehensive paediatric evaluation. With informed parental consent, the extracted tooth was preserved for laboratory analysis to further investigate its microstructural characteristics. For comparative purposes, the specimen was analysed alongside a deciduous tooth obtained from a healthy child, whose parents provided written informed consent for tooth donation. The control tooth was extracted in the absence of pathology, solely due to the natural eruption of its permanent successor despite incomplete root resorption.

Paediatric and genetic evaluation

Upon referral, the child underwent a clinical examination, which showed no signs of genu varum (bowing of the legs). Height and weight were within normal percentiles, and neuromotor development was age-appropriate. Family history revealed that the mother had previously been affected by genu varum due to vitamin D deficiency, which was corrected through supplementation. A comprehensive blood panel (Table 1) revealed markedly low phosphate and vitamin D levels, along with elevated alkaline phosphatase. Serum calcium levels were within the normal reference range. Based on these biochemical abnormalities, vitamin D and calcium supplementation were initiated, resulting in the normalisation of serum vitamin D, and phosphate levels after nine months (Table 1). However, alkaline phosphatase remained elevated. Given the laboratory findings and clinical presentation, particularly the recurrent dental abscesses in the absence of carious lesions, a hereditary form of hypophosphatemic rickets was suspected. Genetic testing targeting commonly affected genes (PHEX, DMP1, ENPP1, FGF23, and SLC34A3) was performed, with negative results for pathogenic variants, effectively excluding the most common forms of hereditary hypophosphatemic rickets. These findings suggest that the underlying condition may be attributed to non-hereditary causes or potentially involve rare genetic variants not included in the standard diagnostic panel.

Histological and microscopic analyses

With parental consent and in compliance with the principles of the Declaration of Helsinki (updated in October 2024), the extracted teeth, case tooth 8.1 and control tooth 8.3, were promptly collected and processed for morphological and chemical analyses. These analyses included micro-computed tomography (micro-CT), scanning electron microscopy (SEM), and energy-dispersive X-ray spectroscopy (EDS). Optical microscopy was performed solely on the case tooth. Two other incisors, 8.2 and 7.1, were extracted due to recurrent abscesses after the start of supplementation therapy and were analysed in the same manner as described above, confirming the findings observed in tooth 8.1.

Micro-CT analysis

The specimens were scanned using a micro-CT system (Skyscan 1176, Bruker, Kontich, Belgium). Prior to scanning, specimens were stored in Falcon vials at 100% relative humidity. Scanning acquisition parameters were set as follows: 80 kV voltage, 300 µA source current, 8.92 µm isotropic voxel size, with a 0.5 mm aluminum plus 0.38-mm copper filter, and a rotation step of 0.5° over 360°, employing frame averaging of 5. Reconstruction was performed using the proprietary software NRecon (Bruker microCT, Kontich, Belgium) with standardised settings, including a 30% beam hardening correction, smoothing level 7 with a Gaussian kernel of 2, ring artifact correction set to 20, and optimised contrast limits based on preliminary scans. Image alignment and reslicing were conducted using Bruker's Viewer software (version 1.5.4.6). Structural differences were clearly observed between the case and control teeth, as illustrated in Figure 2. Compared to the control specimen (Figures 2a, 3a and 4a), the dentine of the case specimen showed irregular mineralisation patterns, with areas of reduced radiopacity and clefts consistent with interglobular dentine (Figures 2b, 3b, and 4b). An enlarged pulp chamber was also noted, frequently containing pulpal calcifications with irregular morphology (Figures 2b and 3b). Increased tooth abrasion was observed in the case tooth, which, associated with the larger pulp space, provided direct contiguity of the pulp space with the oral environment, as is evident in the incisal part.

SEM and EDS analyses

After micro-CT analyses, the specimens were dehydrated, embedded in epoxy resin, and sectioned using a precision saw (Isomet 1000, Buehler, Germany). After cleaning, sections were mounted on conductive stubs with carbon tape and analysed without sputter coating using a tabletop scanning electron

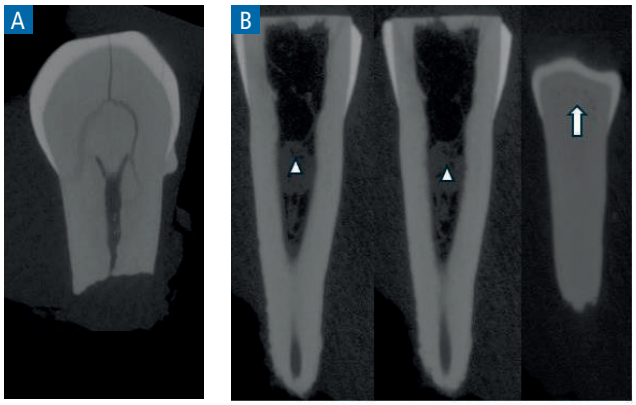

FIG. 2 Coronal micro-CT: A) Control tooth, B) Case tooth showing larger pulp space, pulpal calcifications (triangles) and demineralised dentine structure (arrow). The control tooth displayed linear features resembling fracture lines resulting from initial dehydration. The latter likely occurred during transportation from the dental clinic to the laboratory.

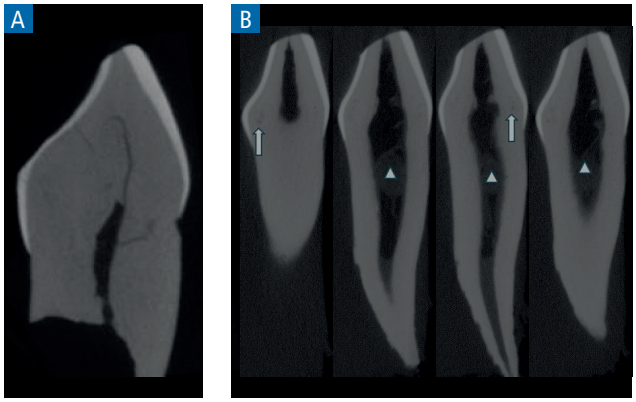

FIG. 3 Sagittal micro-CT: A) Control tooth, B) Case tooth showing pulpal calcifications (triangles) and demineralised dentine structure (arrows).

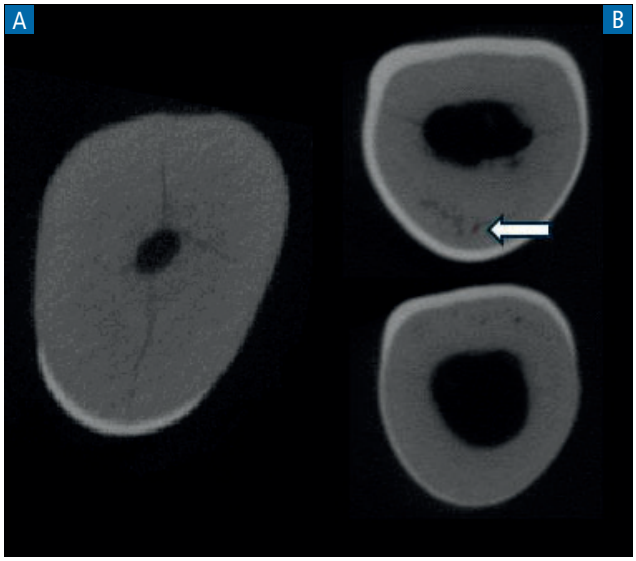

FIG. 4 Axial micro-CT: A) Control tooth, B) Middle and lower coronal sections of the case tooth showing large pulpal spaces and demineralised dentine structure (arrow).

microscope (TM4000Plus, Hitachi, Schaumburg, IL, USA) equipped with an energy-dispersive X-ray spectroscopy (EDS) system (Quantax 75 with XFlash 630H detector, Bruker Nano GmbH, Berlin, Germany). Imaging was conducted in both secondary electron (SE) and backscattered electron (BE) modes at 15 kV under surface-charge reduction mode. BE imaging, which is sensitive to atomic number, enabled differentiation between tissues, with higher atomic number elements (e.g., enamel) appearing brighter than lower atomic number regions (e.g., dentine). Surface morphology was assessed with particular attention to structural features, and three micrographs were captured per field at varying magnifications. EDS analysis was conducted in full-frame mode (300 × 300 µm) with a 150-second acquisition time, and the elemental composition was averaged to reflect weight percentages in the superficial ~1 µm layer. Elemental distribution maps were also generated at 5000× magnification with a 600-second acquisition time. The enamel structure of the case tooth exhibited widespread cracking in multiple directions (Figure 5). Additionally, the enamel surface appeared rough, porous, and disrupted (Figure 6b, 7), in stark contrast to the control tooth (Figure 6a), which displayed the normal, highly organised structure with smooth, well-defined enamel rods. In the control tooth, an adhesive fracture was observed at the interface between the embedding resin and the enamel (Figure 6a), whereas the case tooth exhibited a cohesive fracture within the enamel itself, suggesting decreased mechanical resistance of the tissue. Moreover, the dentino-enamel junction, which is typically characterised by a well-defined and smooth interface, appeared indistinct, irregular, and enlarged in the case tooth, suggesting impaired structural integration between enamel and dentine (Figure 7). SEM analysis revealed the presence of mineralised tissues within the pulp chamber, consistent with pulp stones. As shown in Figure 8, these structures exhibit heterogeneous morphology and irregular distribution.

Line spectrometry analysis of the dentino-enamel junction (DEJ) was conducted to assess mineral distribution across the transition between dentine and enamel in both the case and control teeth. As illustrated in Figure 9, notable differences in mineral gradients across the DEJ were observed, suggesting potential alterations at this crucial interface. Figure 9a, representing the control tooth, shows a gradual,continuous increase in mineral content (primarily calcium and phosphorus) from dentine to enamel. This progressive transition is indicative of a structurally sound DEJ that uniformly distributes mechanical stresses. In

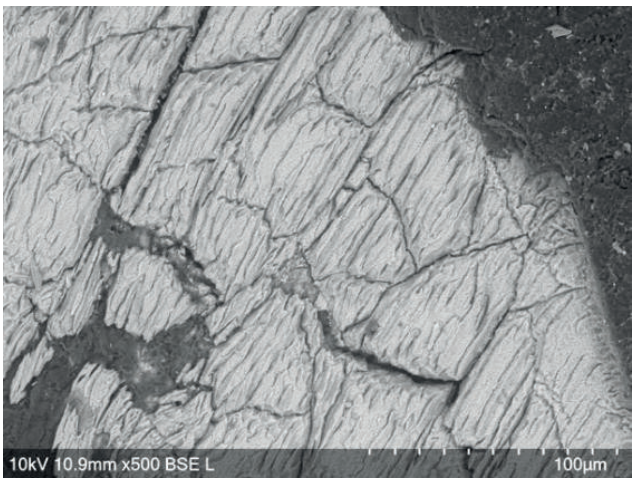

FIG. 5 BSE-SEM image showing the cracks in the enamel structure of the case tooth.

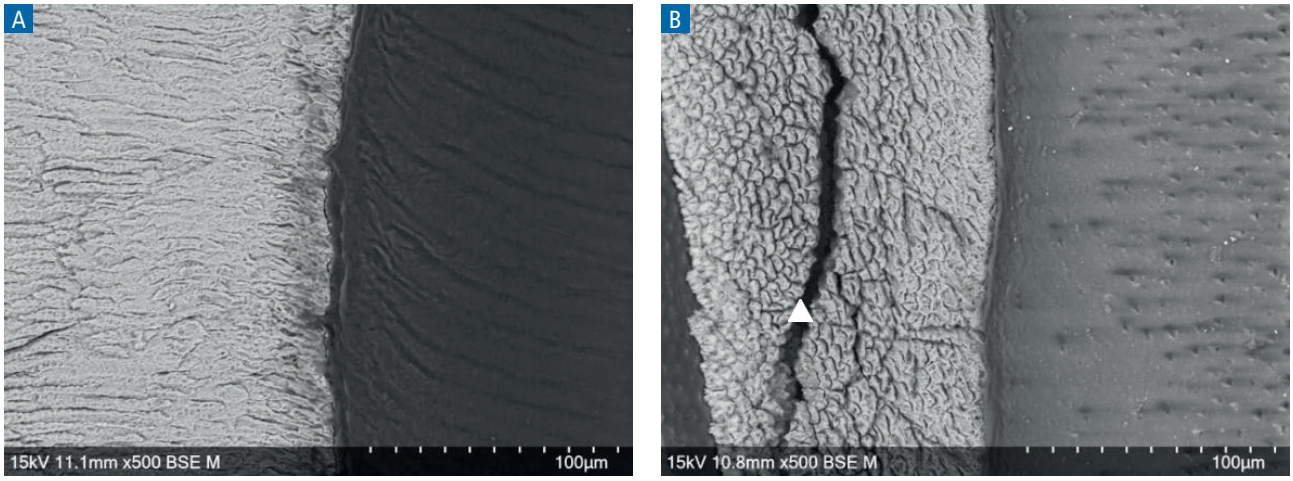

FIG. 6 BSE-SEM: A) Control tooth structure displaying the typical well-organized enamel structure, B) case tooth with porous and uneven enamel and dentin structures. Cohesive fracture is observed within the enamel structure itself (triangle).

contrast, Figure 9b, corresponding to the case tooth, reveals an abrupt shift in mineral composition between dentine and enamel. Such discontinuity may reflect a structurally compromised DEJ, potentially leading to localised stress accumulation and an increased susceptibility to fractures.

Figure 10 presents the EDS analysis of enamel and dentine. In the enamel of the case tooth, pronounced hypomineralisation was observed, particularly in the superficial layer (Figure 10a), where elevated carbon levels were accompanied by a reduction in calcium and phosphorus concentrations compared to the enamel of the control tooth. In contrast, the deep enamel exhibited mineral levels comparable to those of the control tooth. The high carbon content noted in both case and control enamel, as shown in Table 2, is likely due to the embedding of specimens in resin during preparation. Regarding dentine structure (Figure 10b), the case tooth exhibited notable disruptions in mineralisation, with varying mineral concentrations observed across both superficial (mantle) and deep (circumpulpal) dentine layers. The dentine of the control tooth demonstrated the lowest Ca content and Ca/P ratio, establishing a baseline for physiological dentine mineralisation. In the case tooth, both superficial and deep dentine exhibited elevated Ca/P ratios, particularly in the

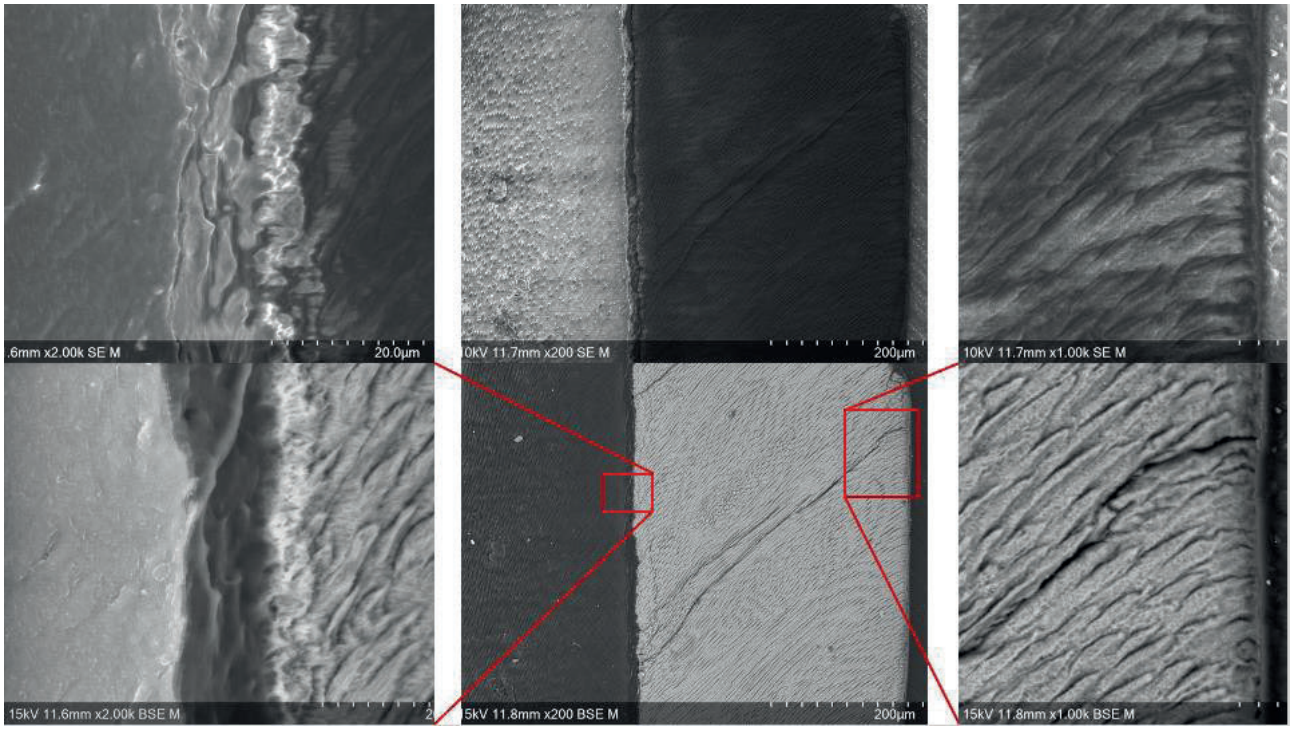

FIG. 7 BSE and SE-SEM images of the case tooth structure showing the dentino-enamel junction. The micrographs at the centre provide a lower-magnification overview of the interface region. The enlargements at the left show the alterations of the DEJ. In particular, the DEJ is enlarged, with an irregular structure and a lower mineral density than both dentine and enamel, as evidenced by a darker grey appearance in BSE mode. The enlargements on the right show the fracture line, which runs mainly parallel to the enamel prisms, occasionally jumping from one interprismatic space to the next, fracturing a prism.

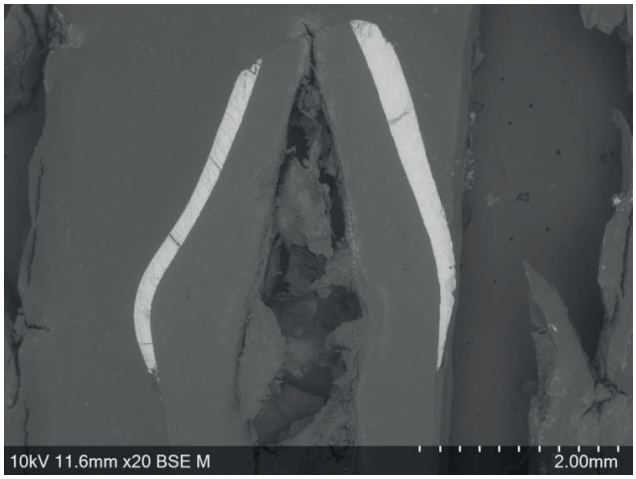

FIG. 8 BSE-SEM image of the case tooth showing extensive mineralised tissue within the pulp chamber, consistent with the presence of pulp stones. As already noted by micro-CT, the incisal part of the tooth is abraded and the upper part of the pulp chamber appears to be in communication with the oral environment, providing a possible entry point for infections and an explanation for the recurrent abscesses.

superficial layer, along with increased Ca and reduced P concentrations, most notably in the deep dentine. Magnesium levels were consistently elevated across all dentine layers in the case tooth. Structurally, mineral distribution was irregular, with superficial dentine displaying higher Ca and P concentrations than the deep dentin. Notably, the mineralised tissues identified as pulp stones showed markedly elevated Ca levels and the highest Ca/P ratio of all regions analysed, suggesting abnormal or pathological (i.e., reactive) mineral deposition.

Optical microscopy and bacterial analysis

For histological analysis, the teeth were initially preserved in a 10% buffered formalin solution (Carlo Erba Reagents, Milan, Italy), followed by decalcification, paraffin embedding, and serial sectioning, as described in previous literature [Giardino et al., 2019; Savadori et al., 2023]. In short, post-fixation decalcification was performed using a 1:1 mixture of 22.5% formic acid and 10% sodium citrate over approximately 3–4 weeks. Afterward, the sample underwent progressive dehydration through graded ethanol baths and was subsequently infiltrated with molten paraffin. Thin sections of 4 µm were obtained from paraffin-embedded blocks using a Leica RM2245 rotary microtome (Leica Biosystems, Nussloch, Germany) and mounted on SuperFrost® adhesive microscope slides (V.W.R. International, Milan, Italy) to ensure optimal adherence. Histological imaging was carried out using an Olympus CX43 light microscope equipped with an

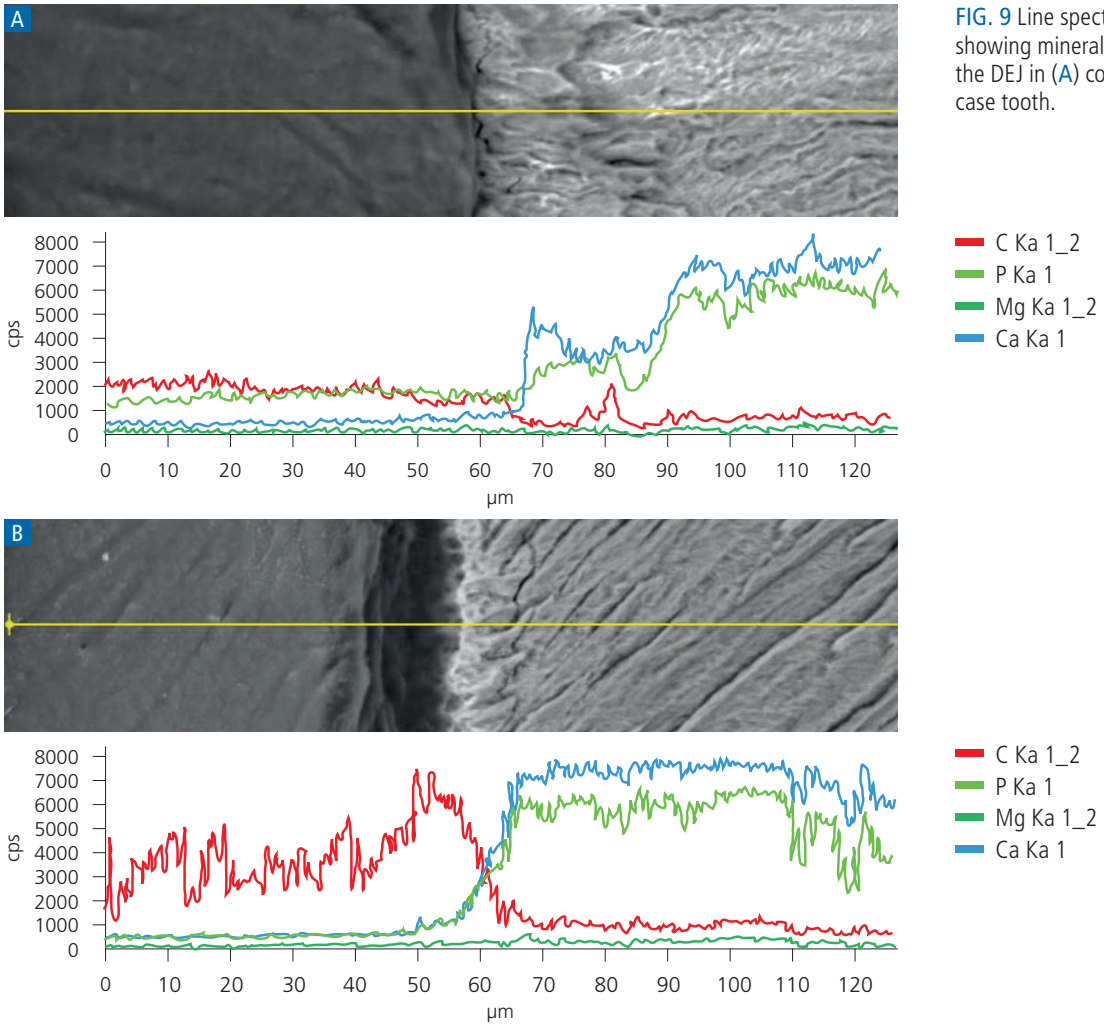

FIG. 9 Line spectrometry showing mineral content across the DEJ in (A) control and (B) case tooth.

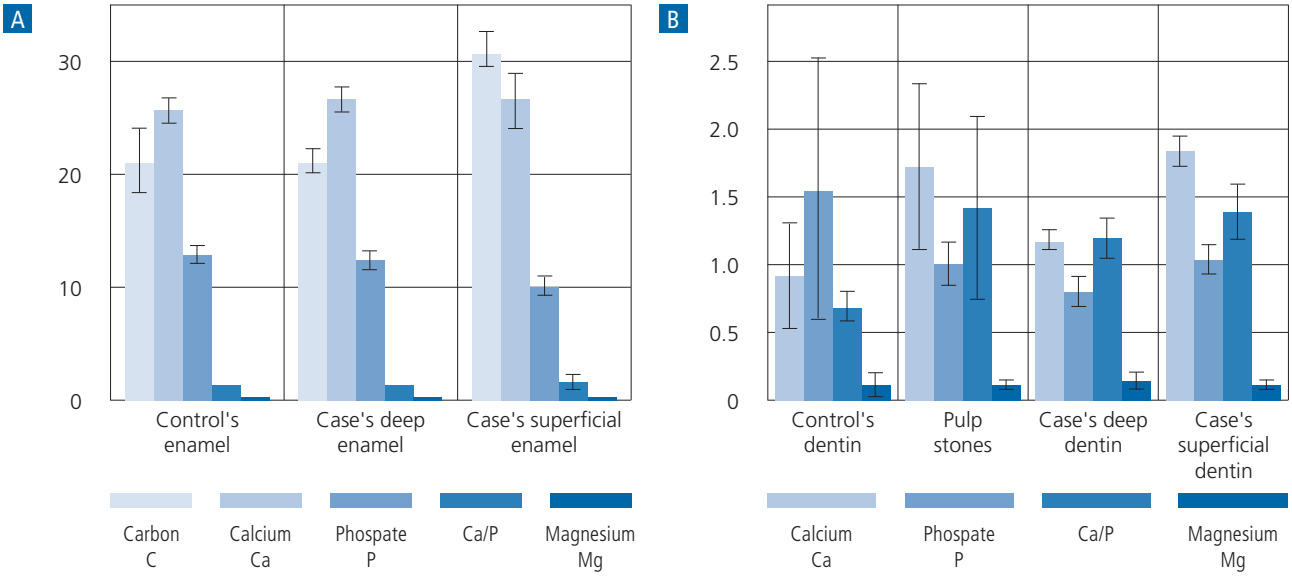

FIG. 10 EDS analysis (mean of 5 randomly chosen points +/- 1 SD) showing the elemental composition of dental tissues from both the case and control teeth A) enamel and B) dentin and pulp stones.

Olympus LC30 color CMOS camera (½ inch sensor, resolution: 2048 × 1532 pixels, pixel size: 3.2 × 3.2 µm; camera adapter: Olympus U-TV0.5XC-3) (Evident-Olympus, Tokyo, Japan), and image processing was conducted via the CellSense software (Evident-Olympus). For high-magnification imaging at 1000× (Olympus 100×/1.25 Oil PlanC N UIS 2, ∞/-/FN22; eyepiece: Olympus WHB10×/20), three sequential captures with varying focal depths were combined to generate a single, sharp image using the Z-stack plug-in in ImageJ (NIH, Bethesda, MD, USA). Additionally, panoramic reconstructions of entire tooth sections were generated by capturing multiple images at 40× magnification (Olympus 4×/0.10 P Plan N UIS 2, ∞/-/FN22; eyepiece: Olympus WHB10×/20) and stitching them together using AutoStitch software [Brown & Lowe, 2007].

At the optical microscopy evaluation, the dentine appears regular along the canal wall, showing a transition from predentine to dentine marked by initial fusion of dentine globules (Figures 11, 12, 13). However, this process remains incomplete, as numerous dentine globules interspersed with interglobular spaces are still clearly visible on the side opposite the canal. As a result, the tooth is characterised by irregular dentine with varying stages of mineralisation. Multiple sites of bacterial infiltration were observed within the dental tissues (Figure 11b and 13). The pulp appears necrotic and disorganised, with visible bacterial colonies in both the pulp chamber and the apical region. Notably, bacteria are also detected within areas of interglobular dentine, which, due to their lower degree of mineralisation, appear more susceptible to bacterial colonisation.

		Enamel	Dentin	Pulp stones
		Weight (%)	Weight (%)	Weight (%)
Structural elements	C	19.47	68.22	65.52
	O	42.61	29.01	30.52
	F	0.00	0.00	0.12
	Cl	0.20	0.11	0.10
	S	0.00	0.40	0.15
	P	12.24	0.73	0.85
	Si	0.02	0.04	0.03
	Al	0.04	0.02	0.05
	Mg	0.19	0.08	0.14
	Na	0.62	0.13	0.10
	K	0.03	0.05	0.13
	Ca	24.57	1.23	2.28
	Total	100.00	100.00	100.00

TAB. 2 Weight % of elements in enamel, dentine and pulp stones of the case tooth.

Discussion

Altered vitamin D levels may or may not respond to supplementation, depending on the underlying aetiology. For instance, in cases of genetic forms of rickets, vitamin D supplementation alone often fails to normalize serum levels or resolve clinical symptoms [Fischer et al., 2023]. In the present case, genetic testing excluded the most common hereditary causes of hypophosphatemic rickets, although rare or unidentified genetic variants cannot be ruled out. Fortunately, the patient responded favourably to vitamin D supplementation, with normalisation of serum vitamin D concentrations. In fact, the maternal origin of the deficiency appears highly plausible, given that the child's mother had previously developed genu varum due to a vitamin D deficiency that was corrected only after delayed supplementation. Multiple studies have demonstrated a strong positive correlation between maternal and neonatal vitamin D status, as maternal vitamin D is transferred to the fetus during gestation. Therefore, maternal deficiency during pregnancy significantly increases the risk of neonatal hypovitaminosis D [Dragomir et al., 2024; Saraf et al., 2016].

Numerous medical conditions have been documented in the literature to impact the development of enamel and dentine, with both disorders themselves and the treatments used potentially influencing this process [Allam et al., 2024; Merglova and Dor, 2020; Samec and Jan, 2022]. Oral manifestations of rickets, both hypophosphatemic and vitamin D–dependent types, are well-documented and often represent some of the earliest clinical signs of the disorder [Baroncelli et al., 2006; Capotosti et al., 2024; Wato et al., 2020]. Among these, recurrent dental abscesses affecting clinically intact teeth, in the absence of carious lesions, are considered hallmark features and serve as valuable early diagnostic clues [Rathore et al., 2013; Souza et al., 2013; Thakur, 2019]. In the present case, the child developed

FIG. 11 Transverse sections of the case tooth: A) specimen stained with hematoxylin and eosin, showing (α) dentine along the canal-facing side and (β) dentine on the external portion of the tooth (scale bar = 1 mm); B) section stained with the Brown-Brenn technique, highlighting (γ) infected necrotic pulp at the level of the pulp horn, (δ) altered dentine containing bacterial colonies, and (ε) the apical third with necrotic pulp infiltrated by bacteria (scale bar = 1 mm).

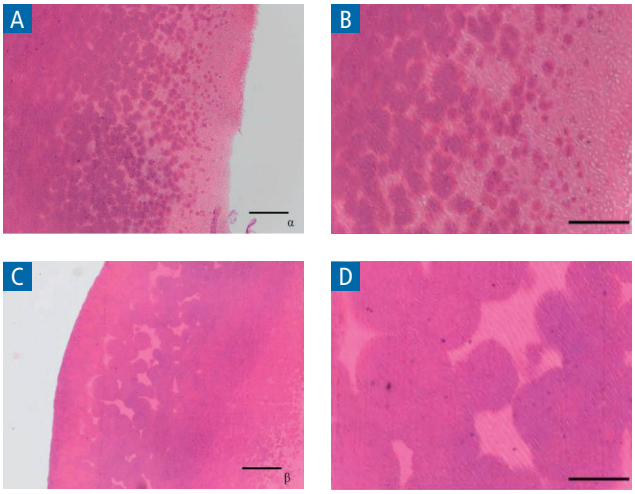

FIG. 12 Higher-magnification views of dentine mineralisation: A) Detail from Figure 11 (α) showing the canal wall with predentine undergoing mineralisation, characterised by clearly visible dentine globules (100×; scale bar = 100 µm); B) Close-up of the dentine globules (200×; scale bar = 50 µm); C) Detail from Figure 11 (β) focusing on the external side of the dentine, where incomplete fusion of globules results in interglobular spaces (100×; scale bar = 100 µm); D) Area illustrating the lack of fusion between globules, leading to the formation of interglobular dentine.

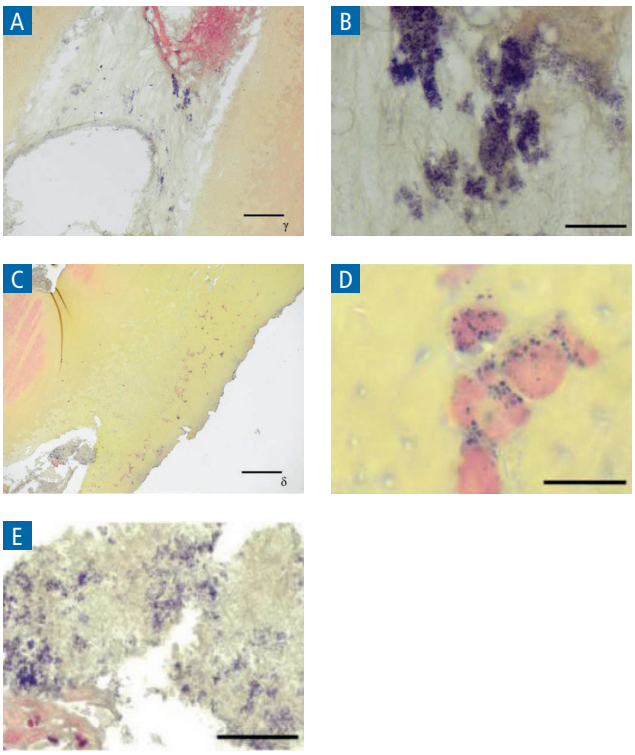

FIG. 13 Degenerative changes in pulp and dentine: A) detail from Figure 11 (γ) showing necrotic pulp within the pulp chamber infiltrated by bacteria (100×; scale bar = 100 µm); B) higher-magnification view of the bacterial infiltration, with cocci-shaped bacteria clearly visible (1000×; scale bar = 50 µm); C) detail from Figure 11 (δ) highlighting dentine with a high concentration of interglobular areas (100×; scale bar = 100 µm); D) interglobular dentine colonised by bacteria (1000×; scale bar = 20 µm); E) detail from Figure 11 (ε) showing the apical third of the pulp in a necrotic state with evident bacterial infiltration (400×; scale bar = 50 µm).

spontaneous dental abscesses involving sound (non-carious) deciduous teeth, which raised clinical suspicion of hereditary rickets. The comprehensive analysis performed on the extracted teeth helped to indicate the increased tooth abrasion, as a consequence of decreased enamel mechanical resistance, coupled with an enlarged pulpal chamber as the most probable cause of dental abscesses. Findings of pulpal stones as reactive mineralisation and bacteria inside the pulp chamber further support this assumption. Although genetic testing excluded common hereditary forms, the dental phenotype closely resembled that observed in genetically determined cases, underscoring the shared impact of impaired mineral homeostasis on dental tissue development and integrity.Micro-CT analyses reported in previous studies of different forms of hereditary rickets have identified dentine hypomineralisation characterised by porosities adjacent to the pulp space, findings consistent with areas of reduced mineral density and interglobular dentine. [Clayton et al., 2021; Ribeiro et al., 2015]. Such features align with the present observations. Furthermore, additional features in the current case include enlarged pulp chambers and pulpal calcifications, likely reflecting dysregulated odontoblastic activity in a mineral-deficient microenvironment. EDS analysis of the pulp stones revealed markedly elevated calcium content and high Ca/P ratios, indicative of excessive or aberrant mineral deposition, in stark contrast to the tightly regulated mineralisation observed in physiological dentine formation.

Optical microscopy and SEM analyses of the case teeth are consistent with findings previously reported in the literature for various forms of rickets [Okawa et al., 2022; Paredes et al., 2018; Soares et al., 2012; Wato et al., 2020]. One hallmark feature was the presence of interglobular dentin, indicative of

impaired mineralisation due to the failure of calcospherite fusion. Additionally, a thick predentine layer was identified, suggesting a delay or arrest at the mineralisation front. SEM imaging further revealed marked structural differences between the case and control teeth. While the control tooth exhibited an adhesive fracture at the enamel- resin interface, the case tooth showed a cohesive fracture within the enamel itself, indicating a significant compromise in the internal structural integrity of the enamel. The enamel, particularly in its superficial layers, displayed clear signs of hypomineralisation. EDS analysis revealed reduced levels of Ca and P, a decreased Ca/P ratio, and elevated carbon content, features consistent with those described in vitamin D-dependent rickets [Liu et al., 2020; Thakur, 2019]. The DEJ appeared disrupted, characterised by sharp fluctuations in mineral levels rather than the smooth and gradual transition typical of healthy teeth. Within the dentin, EDS analysis showed distinct mineral imbalances across different regions: superficial dentine exhibited an increased Ca/P ratio, while deeper dentine demonstrated reduced phosphorus levels, suggesting incomplete or irregular mineralisation. These alterations likely contributed to the formation of interglobular dentine. When compared to existing literature, particularly studies on hypophosphatemic rickets, the present findings exhibit similarities such as the presence of interglobular dentine and localised mineral depletion near the pulp. Whereas many reported cases describe a predominantly affected dentine structure and a relatively preserved enamel and DEJ [Goodman et al., 1998, Seow et al. 1989, Opsahl et al., 2012], the current case showed extensive enamel involvement and disruption of the DEJ. This more widespread pattern likely reflects the systemic effects of vitamin D deficiency on overall mineral metabolism, in contrast to the more localised, genetically mediated phosphate regulation defects characteristic of hypophosphatemic rickets [Carvalho et al., 2020].

In conclusion, this case illustrates how vitamin D deficiency can profoundly disrupt the mineralisation of dental tissues, resulting in enamel hypomineralisation, interglobular dentin, pulpal calcifications, and enlarged pulp chambers. These structural abnormalities compromise tooth integrity, making affected teeth susceptible to spontaneous dental abscesses. Notably, the dental manifestations were among the earliest clinical signs of the underlying systemic disorder, highlighting the critical role of oral findings in the timely diagnosis of metabolic diseases. Despite the inherent limitations of a single-case report with a clinical follow-up of 32 months and the biochemical monitoring of 9 months, the findings highlight the importance of comprehensive dental assessments for early detection and underscore the need for an interdisciplinary approach in paediatric care. Following the initiation of vitamin D supplementation, marked clinical and radiographic improvements were observed.

Competing interest

Authors declare no competing interest in relation to the present study.

Authors contributions

M.G.C, S.C., and C.S examined the patient and decided upon extraction and referral; A.C.I. performed the SEM and EDS analyses; P.S. and V.Z. conducted the optical and bacterial analyses. A.C.I. and A.A. performed the analysis of the results and drafted the manuscript;

M.G.C revised the manuscript. All authors have approved the final version of the manuscript.

Funding

This study received no funding.

Acknowledgments

We are grateful to Dr. Valeria D'Avola for the help in managing the patient, and Dr. Antonella Panio for the help in reviewing the manuscript. The authors acknowledge the support received from the University of Milan through the APC initiative.

Ethical considerations

The study was conducted in compliance with the principles of the Declaration of Helsinki (updated in October 2024). Written informed consent was obtained from the legal guardians of the case and control for publication.

References

› Allam A, Camoni N, Cirio S, Salerno C, Campus G, Cagetti MG. Developmental defects of enamel in childhood cancer survivors: a systematic review and meta-analysis. Eur J Paediatr Dent. 2025;26:131-9.
› Allam A, Cirio S, Elia F, Salerno C, Cagetti MG. Dental manifestations in children affected by hypophosphatemic rickets: a systematic review and meta-analysis. Children (Basel). 2025;12:144.
› Baroncelli GI, Angiolini M, Ninni E, Galli V, Saggese R, Giuca MR. Prevalence and pathogenesis of dental and periodontal lesions in children with X-linked hypophosphatemic rickets. Eur J Paediatr Dent. 2006;7:61-6.
› Brown M, Lowe DG. Automatic panoramic image stitching using invariant features. Int J Comput Vis. 2007;74:59-73.
› Capotosti I, Baroncelli GI, Ligori S, Zampollo E, Giuca MR, Carli E. The care of the patient with X-linked hypophosphatemic rickets. Eur J Paediatr Dent. 2024;25:329-30.
› Carvalho FSR, Feitosa VP, Fonteles CSR, Ribeiro TR, Araújo BS, Ayala AP, et al. Compositional and microhardness findings in tooth affected by X-linked hypophosphatemic rickets. J Clin Exp Dent. 2020;12:e688-94.
› Cashman KD. Global differences in vitamin D status and dietary intake: a review of the data. Endocr Connect. 2022;11:e210282.
› Chanchlani R, Nemer P, Sinha R, Nemer L, Krishnappa V, Sochett E, et al. An overview of rickets in children. Kidney Int Rep. 2020;5:980-90.
› Charoenngam N, Ayoub D, Holick MF. Nutritional rickets and vitamin D deficiency: consequences and strategies for treatment and prevention. Expert Rev Endocrinol Metab. 2022;17:351-64.
› Clayton D, Chavez MB, Tan MH, Kolli TN, Giovani PA, Hammersmith KJ, et al. Mineralization defects in the primary dentition associated with X-linked hypophosphatemic rickets. JBMR Plus. 2021;5:e10463.
› Dragomir RE, Toader DO, Gheoca Mutu DE, Dogaru IA, Răducu L, Tomescu LC, et al. Consequences of maternal vitamin D deficiency on newborn health. Life (Basel). 2024;14:714.
› Durá-Travé T, Gallinas-Victoriano F. Dental caries in children and vitamin D deficiency: a narrative review. Eur J Pediatr. 2024;183:523-8.
› Fischer PR, Johnson CR, Leopold KN, Thacher TD. Treatment of vitamin D deficiency in children. Expert Rev Endocrinol Metab. 2023;18:489-502.
› Giardino L, Grande NM, Savadori P, Del Fabbro M, Plotino G. Clinical and histological findings of post-treatment infection in the presence of vertical root fracture and apical periodontitis: case reports. Eur Endod J. 2019;4:45-8.
› Goodman JR, Gelbier MJ, Bennett JH, Winter GB. Dental problems associated with hypophosphataemic vitamin D-resistant rickets. Int J Paediatr Dent. 1998;8:19-28.
› Haffner D, Leifheit-Nestler M, Grund A, Schnabel D. Rickets guidance: part I—diagnostic workup. Pediatr Nephrol. 2021;37:2013.
› Holick MF, Chen TC. Vitamin D deficiency: a worldwide problem with health consequences. Am J Clin Nutr. 2008;87:1080S-6S.
› Liu AQ, Zhang LS, Guo H, Wu ML, Li TY, Xuan K, et al. Long-term dental intervention and laboratory examination in a patient with vitamin D-dependent rickets type I: a case report. Medicine (Baltimore). 2020;99:e22508.
› Merglova V, Dor J. Developmental enamel defects of primary incisors in preterm infants with very low and extremely low birthweight: a case-control study. Eur J Paediatr Dent. 2020;21:318-22.
› Okawa R, Hamada M, Takagi M, Matayoshi S, Nakano K. A case of X-linked hypophosphatemic rickets with dentin dysplasia in mandibular third molars. Children (Basel). 2022;9:1304.
› Opsahl Vital S, Gaucher C, Bardet C, Rowe PS, George A, Linglart A, et al. Tooth dentin defects reflect genetic disorders affecting bone mineralization. Bone. 2012;50:989-97.
› Paredes SEY, Segato RAB, Moreira LD, Moreira A, Serrano KVD, Rodrigues CT, et al. Dentoalveolar abscesses not associated with caries or trauma: a diagnostic hallmark of hypophosphatemic rickets initially misdiagnosed as hypochondroplasia. Head Neck Pathol. 2018;12:604-9.
› Rathore R, Nalawade TM, Pateel D, Mallikarjuna R. Oral manifestations of vitamin D-resistant rickets in orthopantomogram. BMJ Case Rep. 2013;2013:bcr2012008318.
› Ribeiro TR, Costa FWG, Soares ECS, Williams JR, Fonteles CSR. Enamel and dentin mineralization in familial hypophosphatemic rickets: a micro-CT study. Dentomaxillofac Radiol. 2015;44:20140347.
› Samec T, Jan J. Developmental defects of enamel among Slovenian asthmatic children. Eur J Paediatr Dent. 2022;23:121-4.
› Saraf R, Morton SMB, Camargo CA, Grant CC. Global summary of maternal and newborn vitamin D status: a systematic review. Matern Child Nutr. 2016;12:647-68.
› Savadori P, Dalfino S, Piazzoni M, Parrini M, Del Fabbro M, Tartaglia GM, et al. A simplified method for detecting Gram-positive and Gram-negative bacteria in dental histological samples: a preliminary and comparative study. Acta Histochem. 2023;125:151992.
› Soares ECS, Costa FWG, Ribeiro TR, Alves APNN, Fonteles CSR. Clinical approach in familial hypophosphatemic rickets: report of three generations. Spec Care Dentist. 2013;33:304-7.
› Souza AP, Kobayashi TY, Lourenço Neto N, Silva SMB, Machado MAAM, Oliveira TM. Dental manifestations of patient with vitamin D-resistant rickets. J Appl Oral Sci. 2013;21:601.
› Thakur M. Familial vitamin D-dependent rickets type 2A: a report of two cases with alopecia and oral manifestations. J Oral Maxillofac Pathol. 2019;23:S130-3.
› Van Leeuwen JPTM, Van Driel M, Van Den Bemd GJCM, Pols HAP. Vitamin D control of osteoblast function and bone extracellular matrix mineralization. Crit Rev Eukaryot Gene Expr. 2001;11:199-226.
› Vierucci F, Del Pistoia M, Fanos M, Gori M, Carlone G, Erba P, et al. Vitamin D status and predictors of hypovitaminosis D in Italian children and adolescents: a cross-sectional study. Eur J Pediatr. 2013;172:1607-17.
› Wato K, Okawa R, Matayoshi S, Ogaya Y, Nomura R, Nakano K. X-linked hypophosphatemia diagnosed after identification of dental symptoms. Pediatr Dent J. 2020;30:115-9.